



Kingdom of Saudi Arabia
Imam Mohammad Ibn Saud Islamic University (IMSIU)
Faculty of Science



Eco-Friendly Synthesis of Arabic Gum Coated Iron Oxide Nano Composite For UV-Assisted Water Purification Of Wadi Hanifa

A graduation Project Submitted to the Department of Physics in Partial
Fulfillment of the requirements

For the degree of Bachelor of Science in Applied Physics

By

Seham Al-Anazi

Taif Al-Awwad

Supervisor by:

Dr. Nawal Madkhali

IMSIU- Riyadh -KSA

Table of Contents

List of Figures.....	I
List of Tables	II
Abstract :.....	III
الملخص العربي.....	IV
Chapter 1: General Introduction.....	1
1.1 Fundamentals of Magnetism in Nanoparticles	1
• Magnetic Dipoles	2
• The Magnetic Induction	3
• Permeability	3
• Susceptibility.....	3
1.2 Classification of Magnetic Nanoparticles:.....	4
• Diamagnetism	4
• Paramagnetism:	5
Ferromagnetism:	6
• Anti-Ferromagnetism:	6
• Ferrimagnetism:.....	7
1.3 Hysteresis loop	9
1.4 Applications of Magnetic Nanoparticles (MNPs).....	11
Chapter 2 Methodology	12
2.1 Sample preparation:	12
2.2 Vibrating-Sample Magnetometer (VSM) Device	12
2.2. Ball Milling	14
2.3. Fourier-transform infrared (FTIR) spectroscopy	15
Chapter 3 Results and discussion	16
3.1 Fourier-transform infrared (FTIR)	16
3.2 Magnetic properties and Langevin Fit	17
3.3 Photo degradation of Pollutants in <i>Wadi Hanifa</i> water :.....	20
Conclusion.....	22
References	23

List of Figures

Figure:(1.1): Magnetic field lines of force around a current loop and a bar magnet.....	2
Figure (1.2): No dipoles exist (left), and dipoles are induced aligned opposite to field direction (right).....	4
Figure (1.3): randomly oriented no net magnetization (left) and preferentially oriented along field direction (right).....	4
Figure (1.4): mutual alignment of atomic dipoles.....	5
Figure. (1.5): These Mn^{2+} ions are arrayed in the crystal structure such that the moments of adjacent ions are antiparallel.....	6
Figure. (1.6): the spin magnetic moment configuration for Fe^{2+} and Fe^{3+} ions in Fe_3O_4	7
Figure (1.7): The hysteresis loop.....	8
Figure (2.1): scheme and photo of the designed VSM.....	9
Figure. (2.2): Schematic diagram for the preparation of nano alloys using ball milling.....	14
Figure. (2.3): photo of designed FTIR.....	15
Figure. (2.4): scheme and photo of the designed photo degradation setup.....	16
Figure (3.1). The FTIR analysis.....	17
Figure (3.2) Langevin fit steps in origin lap.....	19
Figure (3.3) Hysteresis loop.....	19
Figure. (3.4). UV spectra and photo degradation percent of samples.....	21

List of table

Table1.1 Magnetic parameters, relation and SI-unit.....	4
Table 3.1: Magnetic properties of Fe_2O_3 and Arabic gum samples.....	18

Abstract :

In this project, we investigated the magnetic properties using Vibrating Sample Magnetometer at room temperature and analyzed the structural properties using Fourier transform infrared spectroscopy(FTIR).The two samples studied were iron oxide (Fe_2O_3) and iron oxide doped with Arabic gum polymer. We prepared a composite material consisting of both samples in a 2:3 ratio using the mechanical ball milling method for 30 minutes. The resulting composite was then applied to study the purification of *Wadi Hanifa* water after exposure to ultraviolet (UV) radiation for different durations: 0, 30, 60, 90, 120, and 180 minutes. We examined the absorption properties of both the pure iron oxide sample and the Arabic gum-doped sample for their efficiency in water absorption and purification.

الملخص العربي

في هذا المشروع، قمنا بدراسة الخصائص المغناطيسية للعينات باستخدام مقياس الاهتزاز المغناطيسي (VSM) في درجة حرارة الغرفة، بالإضافة إلى تحليل الخصائص التركيبية باستخدام مطياف تحويل فورييه للأشعة تحت الحمراء (FTIR). تمت دراسة عينتين رئيسيتين، وهما: أكسيد الحديد (Fe_2O_3) وأكسيد الحديد المشوب ببوليمر صمغ العربي تم تحضير مادة مركبة من العينتين بنسبة 3:2 باستخدام تقنية الطحن الكروي الميكانيكي لمدة 30 دقيقة. بعد ذلك، تم استخدام هذه المادة المركبة لدراسة كفاءتها في تنقية مياه وادي حنيفة، بعد تعريضها لأشعة فوق البنفسجية (UV) لفترات زمنية مختلفة: 0، 30، 60، 90، 120، و180 دقيقة. وقد تم تحليل خصائص الامتصاص لكلا العينتين (العينة النقية والمشوبة) باستخدام مطيافية UV-Vis، لتقييم كفاءتهما في امتصاص وتنقية المياه بعد التعرض للأشعة فوق البنفسجية.

الاهداء

ها نحن نصل اليوم إلى محطة الختام، بعد سنواتٍ من السعي والمثابرة، والتعب الذي رافقته آمال لا تنطفئ.... تم بحمد الله هذا البحث، فله الحمد أولاً وآخرًا، ظاهرًا وباطنًا، عدد ما كان وعدد ما يكون.

نهدي ثمرة هذا الجهد المتواضع...إلى من كانا أول الحكاية، ونورها، وظلها الوارف، إلى من لولا هما – بعد الله – ما كنا، ولا وصلنا، ولا نهضنا من كل تعب . إلى من نحبهما حبًا لا يُضاهى، ونحمل لهما في قلوبنا من الدعاء ما لا يبلغه الكلام، إلى من علّمانا أن الإصرار بداية النجاح، وأن العلم ميراث لا يفنى، إلى والدينا الحبيبين، وإلى كل يدٍ امتدت بخير، وكل قلبٍ دعا لنا في الغيب، وكل روحٍ رافقتنا بمحبة صادقة...إلى أولئك الذين كانوا النور حين أظلمت المسارات... نهدي إليكم عرفاننا وامتناننا العميق.

وإلى من كانت خلف هذا العمل علمًا وصبرًا وتوجيهًا، إلى من أعطت بسطاء، وسعت بإخلاص الدكتوراة / نوال مدخلي شكرًا من القلب، فلولاً دعمك وتوجيهك لما اكتمل هذا الجهد .

سهام وظيف
19May 2025

Chapter 1: General Introduction

1.1 Fundamentals of Magnetism in Nanoparticles

Magnetism arises from the motion of electrically charged particles, such as electrons, whose intrinsic spin and orbital angular momentum generate microscopic magnetic moments. In bulk materials, these moments align in domains, producing macroscopic magnetization. However, at the nanoscale (particles < 100 nm), quantum mechanical effects dominate, leading to unique magnetic behaviors. Nanoparticles lack the multi-domain structures of bulk materials, often exhibiting single-domain states. Superparamagnetic occurs when thermal energy overcomes the magnetic anisotropy energy, causing spontaneous randomization of magnetic moments in the absence of an external field. This phenomenon prevents permanent magnetization and is highly size-dependent, as smaller particles have lower energy barriers between spin states. Additionally, surface effects become critical in nanoparticles: a larger surface-to-volume ratio increases the proportion of atoms with disordered spins, reducing overall magnetization compared to bulk counterparts. Finite-size effects also influence magnetic anisotropy, coercivity, and susceptibility, which are tunable by controlling nanoparticle size, shape, and composition (e.g., iron oxide, cobalt, or nickel nanoparticles). Understanding these fundamentals is pivotal for designing nanoparticles with tailored magnetic properties for advanced applications. The magnetic field distributions as indicated by lines of force are shown for a current loop and a bar magnet as shown in Figure (1.1).

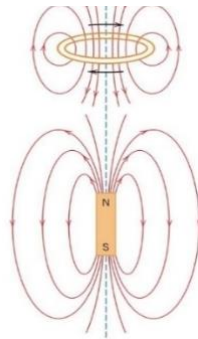


Figure:(1.1): Magnetic field lines of force around a current loop and a bar magnet[1]

- **Magnetic Dipoles**

Magnetic forces are generated by moving electrically charged particles; these magnetic forces are in addition to any electrostatic forces that may prevail. Magnetic dipoles may be thought of as small bar magnets composed of north and south poles instead of positive and negative electric charges. It's quantified by its magnetic moment: $I \times A$, where I is the current loop's current and A is the loop's area. For nanoparticles, the magnetic moment arises from the collective alignment of electron spins and orbital motions. In single-domain nanoparticles (e.g., iron oxide), all atomic magnetic moments align coherently, creating a net dipole moment.

Superparamagnetic nanoparticles exhibit fluctuating dipole orientations due to thermal agitation.[2]

- **The Magnetic Induction**

The magnetic induction or magnetic flux density represents the magnitude of the internal field strength within a substance that is subjected to an magnetic field strength. Both magnetic flux density and magnetic field strength are field vectors, being characterized not only by magnitude, but also by direction in space[1].

- **Permeability**

A property of the specific medium through which the magnetic field strength passes. The permeability or relative permeability of a material is a measure of the degree to which the material can be magnetized, or the ease with which a magnetic flux density can be induced in the presence of an external magnetic field strength.

- **Susceptibility**

Magnetic susceptibility (denoted as χ) is a dimensionless proportionality constant that quantifies how much a material becomes magnetized in response to an applied magnetic field. It describes the material's intrinsic tendency to acquire magnetization (when exposed to a magnetic field strength. Table(1.1) shown the relationship between magnetic parameters and SI units.

Quantity	Symbol	Relationship	SI-Unit
Magnetic induction	B_0	$B_0 = \mu_0 H$	Tesla
Magnetic field strength	H	$H = \frac{NI}{L}$	A/m
Magnetization	M	$B = \mu_0 H + \mu_0 M$ $M = \chi_m H$	A/m
Permeability of a vacuum	μ_0	$B = \mu_0 H$	T·m/A.
Relative permeability	μ_r	$\mu_r = \frac{\mu}{\mu_0}$	Unitless
Susceptibility	χ_m	$\chi_m = \mu_r - 1$	Unitless

Table1.1 Magnetic parameters ,relation and SI-unit

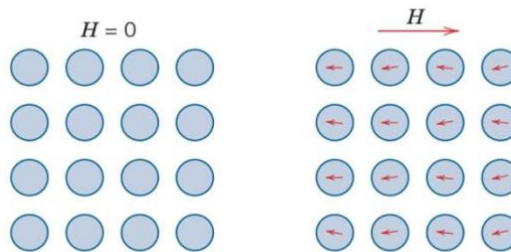
1.2 Classification of Magnetic Nanoparticles:

The types of magnetism include diamagnetism which is weak, opposing field), paramagnetism which is weak, aligned with field), and ferromagnetism which is: strong, persistent, alignment. Subclasses like antiferromagnetism: which cancel spins and ferrimagnetism: equal antiparallel spins arise from competing dipolar interactions. All materials exhibit at least one type, with behavior governed by electron spin/orbital dynamics and atomic dipole alignment under external fields.

- **Diamagnetism**

- ✓ Is a very weak form of magnetism that is nonpermanent.
- ✓ Magnetic susceptibility is negative and The volume susceptibility χ_m for diamagnetic solid materials is on the order of 10^{-5} .
- ✓ The relative permeability μ_r is less than unity (however, only very slightly). The atomic dipole configuration for a diamagnetic material with and without a magnetic field. In the absence of an

external field, no dipoles exist, in the presence of a field, dipoles are induced that are aligned opposite to the field direction as shown in Figure(1.2)



Figure(1.2):No dipoles exist (left) and dipoles are induced aligned opposite to field direction (right).[2]

- **Paramagnetism:**

- ✓ The exhibit magnetization only when in the presence of an external field.
- ✓ Relative permeability μ_r that is greater than unity.
- ✓ configuration with and without an external magnetic field for a paramagnetic material in Figure . (1.3).
- ✓ Relatively small but positive magnetic susceptibility. Susceptibilities for paramagnetic materials range from about 10^{-5} to 10^{-2} . The Atomic dipole

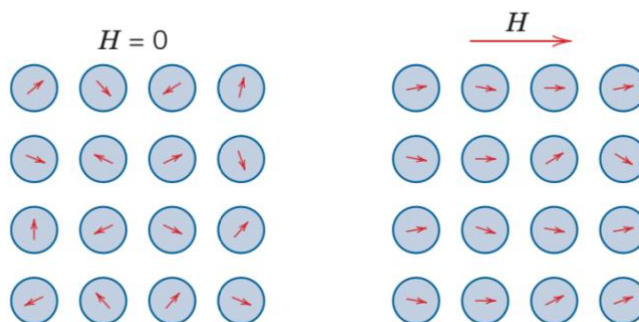


Figure . (1.3): paramagnetic material

Ferromagnetism:

- ✓ Certain metallic materials possess a permanent magnetic moment in the absence of an external field, and manifest very large and permanent magnetizations.
- ✓ Magnetic susceptibilities large and positive as high as 10^6 .
- ✓ The maximum possible magnetization, or saturation magnetization M_s , of a ferromagnetic material represents the magnetization that results when all the magnetic dipoles in a solid piece are mutually aligned with the external field. For Schematic illustration of the mutual alignment of atomic dipoles for a ferromagnetic material, which will exist even in the absence of an external magnetic field as in Figure. (1.4)

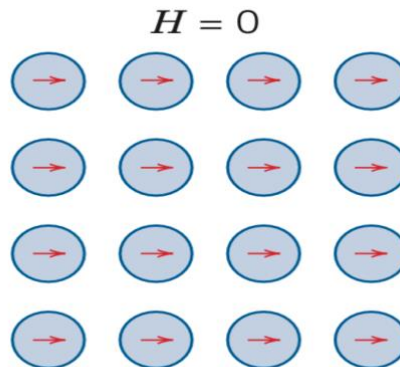
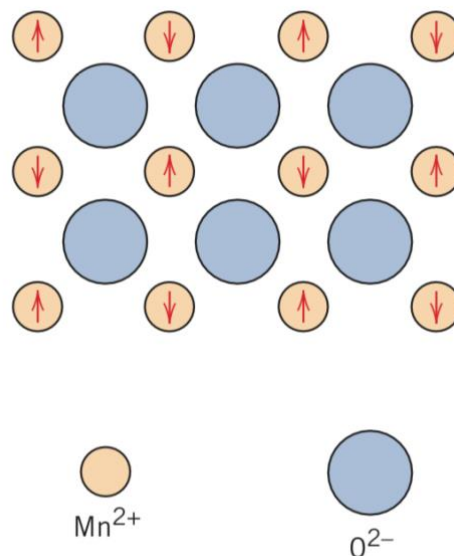


Figure (1.4): mutual alignment of atomic dipoles. [1]

- **Anti-Ferromagnetism:**

- ✓ phenomenon of magnetic moment coupling between adjacent atoms.
- ✓ alignment moments of neighboring atoms or ions in exactly opposite directions.

- ✓ the opposing magnetic moments cancel one another and, as a consequence, the solid as a whole possesses no net magnetic moment. Manganese oxide (MnO) is one material that displays this behavior. This arrangement is represented schematically in Figure . (1.5). [1]



- Figure .(1.5): These Mn^{2+} ions are arrayed in the crystal structure such that the moments of adjacent ions are antiparallel. [1]
- **Ferrimagnetism:**
 - ✓ Some ceramics also exhibit a permanent magnetization.
 - ✓ the net ferrimagnetic moment arises from the incomplete cancellation of spin moments.
 - ✓ the antiparallel coupling of adjacent iron ions.
 - ✓ the spin moments of all Fe^{3+} ions cancel one another and make no net contribution to the magnetization of the solid.
 - ✓ All the Fe^{2+} ions have their moments aligned in the same direction.
 - ✓ The saturation magnetizations for ferrimagnetic materials are not as high as for ferromagnets.

With this inverse spinel structure, half the trivalent Fe^{3+} ions are situated in octahedral positions, the other half, in tetrahedral positions. The divalent Fe^{2+} ions are all located in octahedral positions. The critical factor is the arrangement of the spin moments of the Fe ions, as represented in Figure .(1.6). [1]

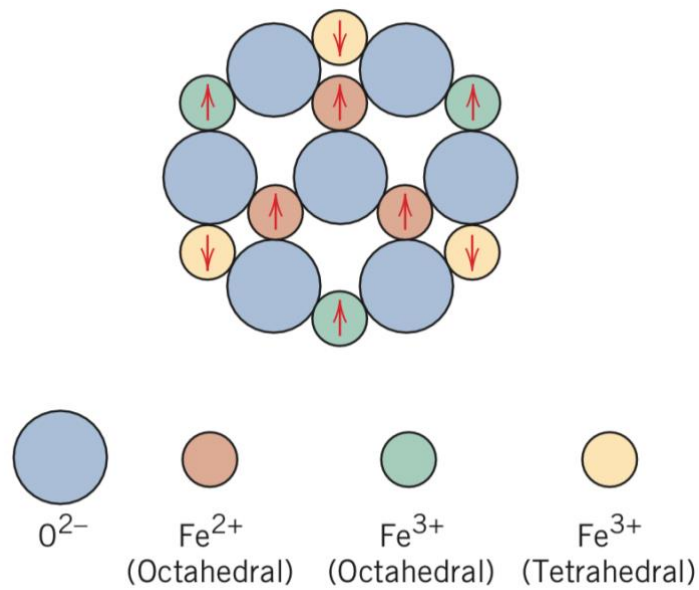
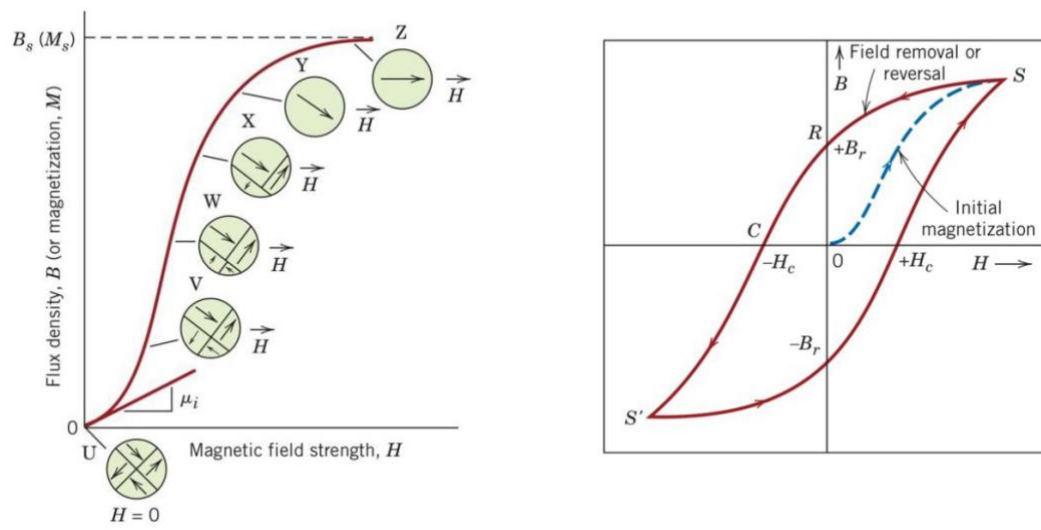


Figure .(1.6): the spin magnetic moment configuration for Fe^{2+} and Fe^{3+} ions in Fe_3O_4 . [1]

1.3 Hysteresis loop

The hysteresis loop is a graphical representation of the relationship between the magnetization of a material and the external magnetic field applied to it. It illustrates how the magnetization of a magnetic material changes as the magnetic field is increased and then decreased. Here are the key points:

- 1) Flux density B and field intensity H are not proportional for ferromagnets and ferrimagnets .
- 2) If the material is initially unmagnetized, then B varies as a function of H as shown in Figure .(1.7).(left).The curve begins at the origin, and as H is increased, the B field begins to increase slowly, then more rapidly, finally leveling off and becoming independent of H .
- 3) As an H field is applied, the domains change shape and size by the movement of domain boundaries.
- 4) A hysteresis effect is produced in which the B field lags behind the applied H field, or decreases at a lower rate. Magnetic flux density versus the magnetic field strength for a ferromagnetic material that is subjected to forward and reverse saturations (points S and S'). The hysteresis loop is represented by the solid curve; the dashed curve indicates the initial magnetization. The remanence B_r and the coercive force H_c are also shown in Figure .(1.7).(right). [1]



Figure(1.7):The hysteresis loop [2]

1.4 Applications of Magnetic Nanoparticles (MNPs)

Magnetic nanoparticles exhibit unique physical and chemical properties, making them suitable for a wide range of applications in different fields.

These include:

- Medical Applications:
 - MRI contrast agents.
 - Targeted drug delivery using external magnetic fields.
 - Hyperthermia therapy for cancer treatment (heating tumor cells to enhance treatment response).
- Electronics and Data Storage:
 - Increasing capacity and performance of magnetic storage devices.
 - Enhancing spintronics technologies.
 - Use in giant magneto-resistance (GMR) sensors.
- Environmental Applications:
 - Water purification by adsorbing pollutants and easy magnetic separation.
 - Reusability reduces cost and environmental impact.
- Industrial and Catalytic Applications:
 - Use in magnetic fluids for cooling and damping.
 - Catalysts in chemical reactions.
- Challenges and Solutions:
 - Precise control of particle size and magnetic stability is essential.
 - Protection against oxidation by coatings such as starch, dextran, and PEG-Polymers.

Chapter 2| Methodology

2.1 Sample preparation:

Two samples of iron oxide were used in this study: the first is pure iron oxide(Fe_2O_3), referred to as (R), and the second is iron oxide doped with Arabic gum, referred to as (RW) with ratio 2:3. The compounds were obtained from Sigma-Aldrich, and all measurements were conducted on the samples in their pure form and powder state.

2.2 Vibrating-Sample Magnetometer (VSM) Device

Magnetic properties of the two samples have been measured at room temperature (300K) by used Vibrating-sample magnetometer (VSM) scheme of the system is depicted in and follows the configuration of the classical VSM. We weighed 25 mg of each material — pure Arabic gum and iron oxide obtained from Sigma-Aldrich, and placed them at the center of the sample holder, as illustrated in the figure(2.1). This setup was prepared to measure the magnetic properties of the two materials using a Vibrating Sample Magnetometer (VSM). In this method, the sample is positioned precisely in the middle of the holder and vibrated within a high-frequency magnetic field. As the sample vibrates, the magnetic flux changes, causing the material to become magnetized. The VSM then measures the resulting magnetization, producing a hysteresis curve for each material.

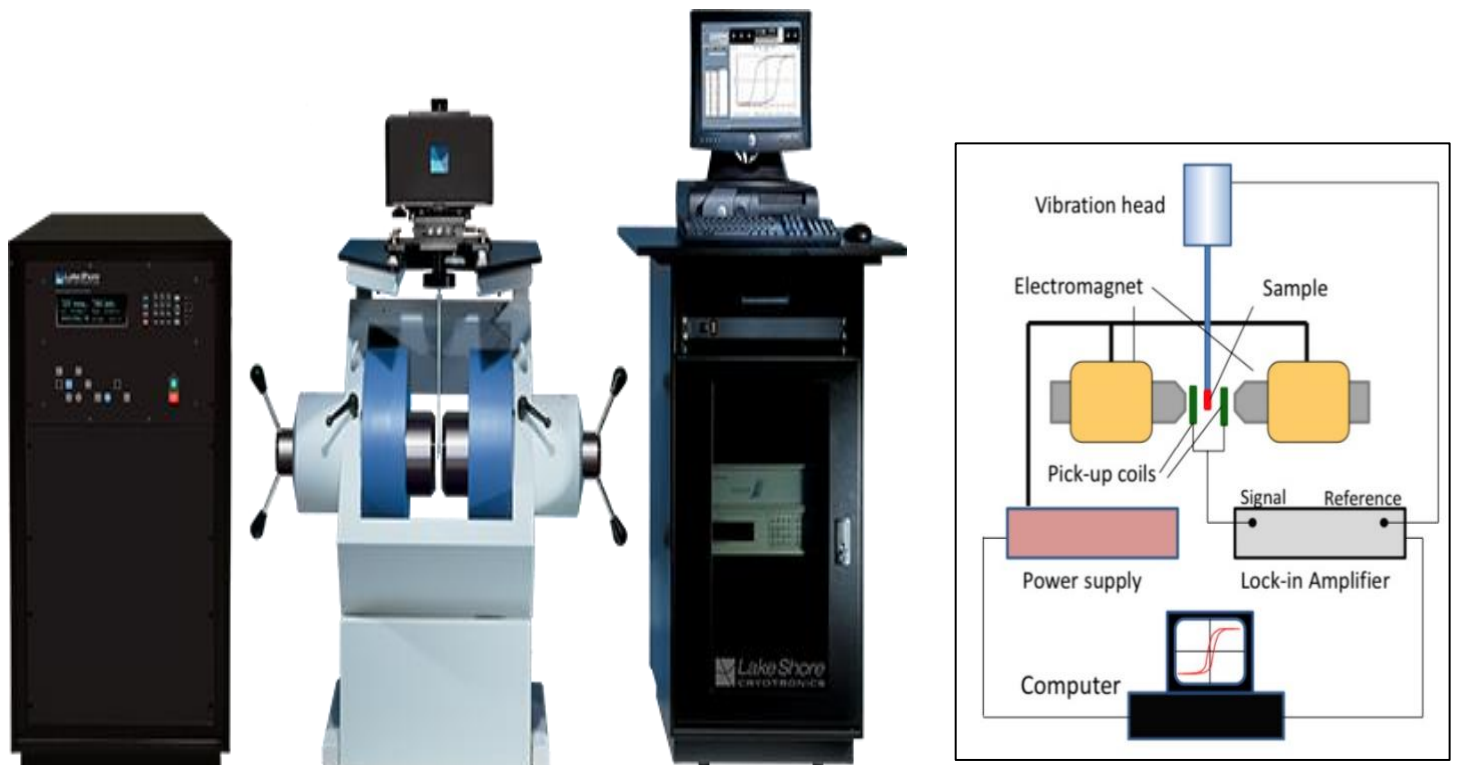


Figure (2.1): scheme and photo of the designed VSM

2.2. Ball Milling

Ball milling is a widely used mechanical process for grinding, blending, and modifying materials at the micro- and nanoscale. It is employed across various fields, including materials science, chemistry, metallurgy, and nanotechnology. [3]. Ball milling involves placing materials in a rotating cylindrical chamber as shown in Figure. (2.2). partially filled with grinding media—typically steel, ceramic, or tungsten carbide balls. The balls impact and grind the materials, causing particle size reduction, mixing, and sometimes initiating chemical reactions. In this case the composite samples (Arabic gum/ Fe_2O_3) have a speed 350rpm for 30 min.



Figure.2.2: Schematic diagram for the preparation of nano alloys using ball milling

2.3. Fourier-transform infrared (FTIR) spectroscopy

Infrared spectral data were collected using an Agilent Cary 630 FTIR spectrometer. This device utilizes a Michelson interferometer and operates over a wavenumber range of 400-4000 cm^{-1} . Figure. (2.3).



Figure.2.3: photo of the designed FTIR

2.4. Photo degradation setup

A photo-degradation setup is a laboratory system used to study how pollutants or chemical compounds break down when exposed to light, especially UV (ultraviolet) or visible light. It is commonly used to test the effectiveness of photocatalyst, such as nanoparticles, in water purification or environmental remediation. Figure. (2.4).

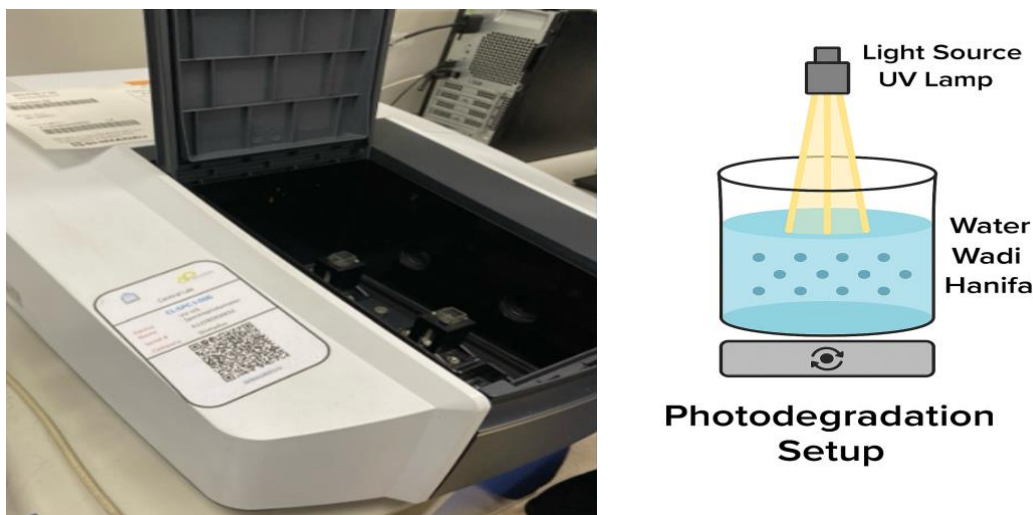


Figure.2.4: scheme and photo of the designed photo degradation Setup

Chapter 3| Results and discussion

3.1 Fourier-transform infrared (FTIR)

Figure.(3.1). The FTIR analysis indicates significant changes in the vibrational characteristics of Fe_2O_3 upon doping with Arabic gum. The removal of specific peaks and the emergence of new bands suggest interactions that alter the chemical environment, impacting the properties of the composite. The spectrum shows a distinct peak around 468 cm^{-1} . At $\text{Fe}_2\text{O}_3/\text{Arabic Gum}$ Composite sample: The peak at 468 cm^{-1} is significantly diminished or entirely removed in the presence of Arabic gum. The removal of the 468 cm^{-1} peak suggests that the Arabic gum interacts with the iron oxide, potentially forming new bonds (Fe-O-O) or altering the existing Fe-O bonding environment. For Fe_2O_3 sample: In the range $1000\text{-}1200\text{ cm}^{-1}$: Stretching vibrations of Fe-O bonds are noted, indicating stable bonding in the iron oxide. Between $1600\text{-}3500$

cm⁻¹:C=O and C-H Bonds: Peaks in this region may correspond to functional groups present in Arabic gum.

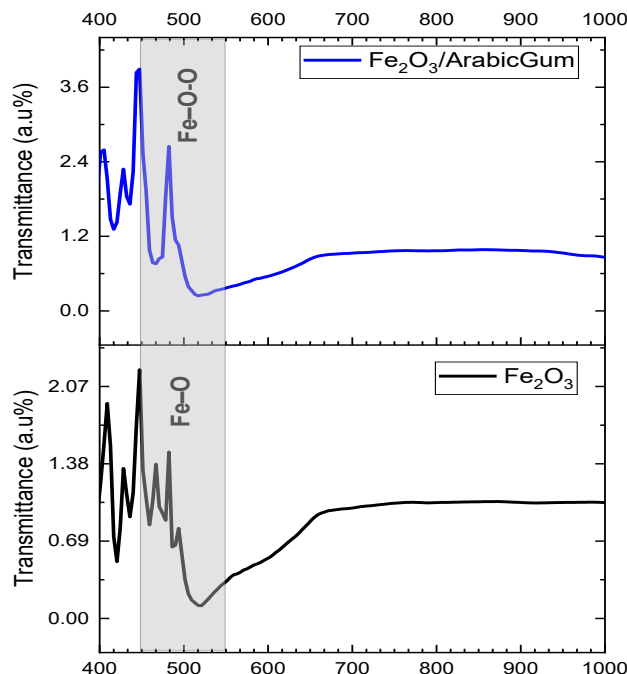


Figure.(3.1). The FTIR analysis

3.2 Magnetic properties and Langevin Fit

Magnetization-field ($M - H$) curves recorded at 300 K for samples, are shown in Figure 3.3. It can be seen from the VSM curves: superparamagnetic behavior of all samples. The saturation magnetization (M_s), coercivity (H_c), and remanence (M_r) for all samples at different temperatures are presented in Table 3.1. Using a vibrating sample magnetometer (VSM) at room temperature 300 K, the magnetic properties of material were examined from -10,000 to 10,000 G, and the result is shown in Figure 3.3. We made drawings normalized, the normalization means dividing by the mass weight in(g). and we found value of M_s , M_r ,

and H_c at it is in the table and comparing with other references. To know the behavior of the material, we calculated the magnetic susceptibility from the figure, by calculating the slope of the curve based on the mathematical formula that describes the magnetism of the material with the applied magnetic field. Where $M = \chi H$ and χ : Magnetic Susceptibility of sample, H : Applied Magnetic field, M : Magnetization of sample (emu/g). We determined the coercivity, remanence, and saturation magnetization for our samples: The magnetic parameters were evaluated before and after applying the Langevin fit, and the results are summarized in the table(3.1). We added the Langevin fit in the Origin lap using the nonlinear curve fit tool, we defined the Langevin fit in the function box as shown in Figure 3.2:

$$M(H) = M_s \left(1 - \frac{b}{H^2} \right)$$

We used it describes the magnetization near the saturation where M_s represents the saturation magnetization and b is a fitting parameter related to the material's magnetic properties.

Material	H_c (A/m)	M_r (emu/g)	M_s (emu/g)		χ	μ_r	Type
			Experiment	Langevin fit			
Fe_2O_3	1.9×10^{-2}	3.8×10^{-3}	1.043	1.029	6×10^{-4}	1.00006	superparamagnetic
Arabic gum	1.8×10^{-2}	3×10^{-3}	0.081	0.095	7×10^{-5}	1.00007	superparamagnetic

Table 3.1: Magnetic properties of Fe_2O_3 and Arabic gum samples

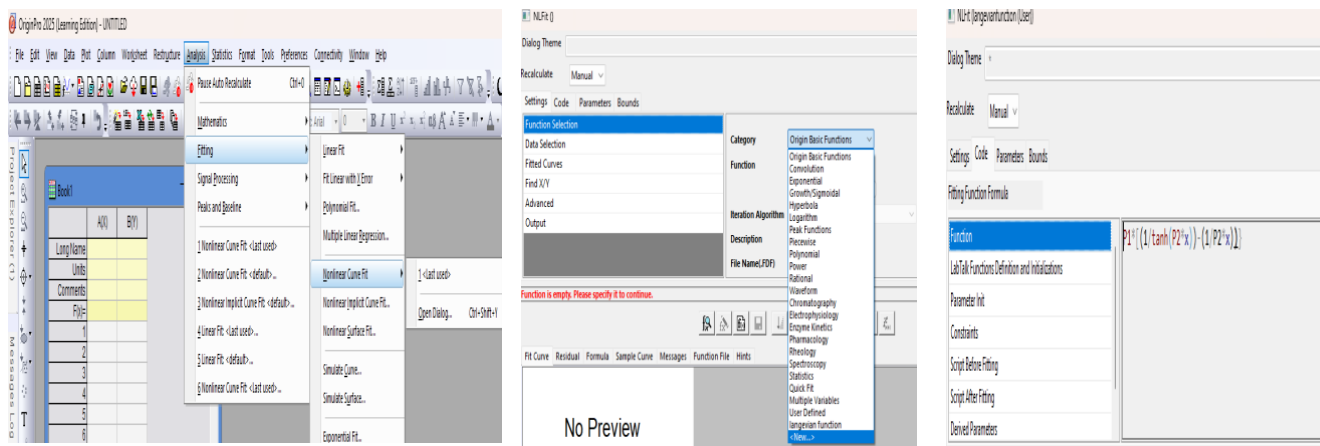


Figure 3.2 Langevin fit steps in origin lab

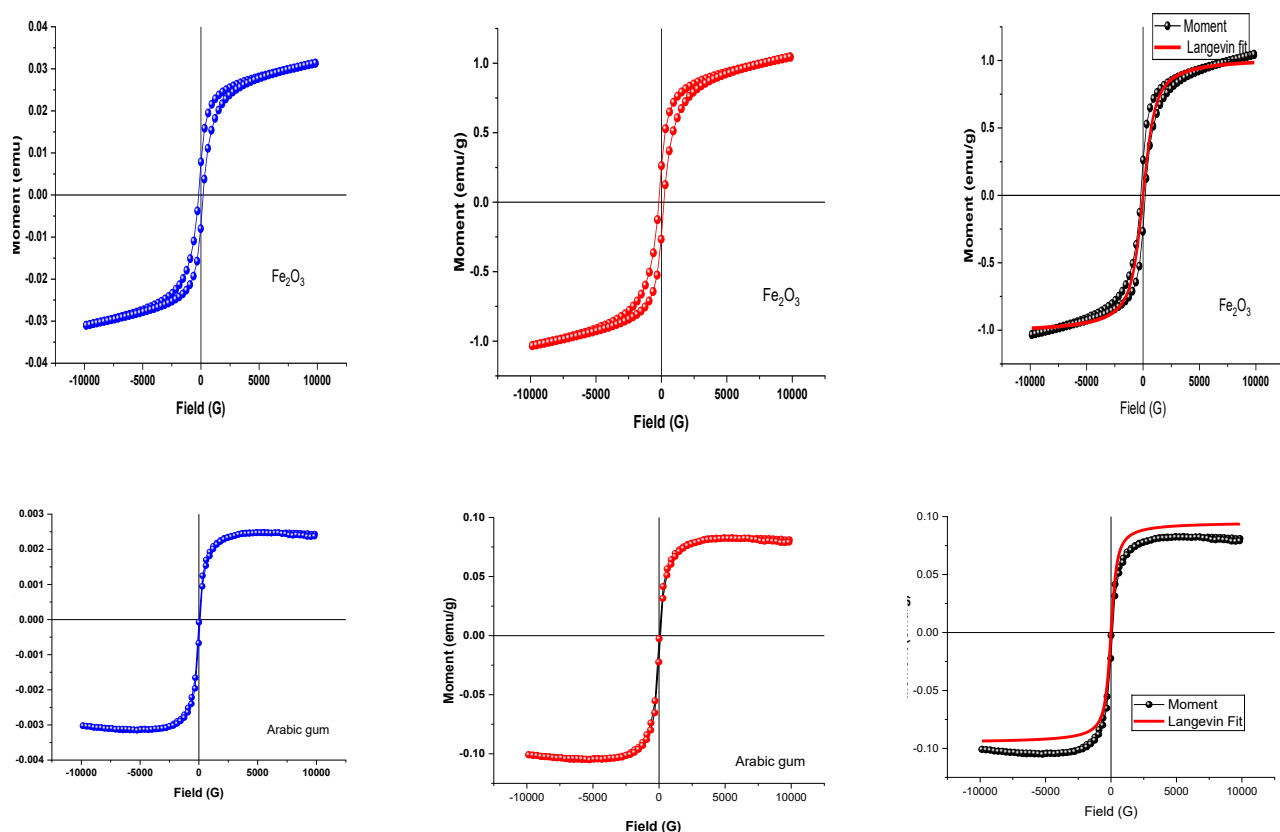


Figure 3.3 Hysteresis loop

3.3 Photo degradation of Pollutants in *Wadi Hanifa* water :

In this part of the research, we utilized magnetic materials after preparing a composite mixture of them using the ball milling method. We studied the photo degradation of the two samples under ultraviolet (UV) light at six different exposure times: 0, 30, 60, 90, 120, and 180 minutes, using a water sample from *Wadi Hanifa*. We analyzed the absorption rate, which increased with UV (uv lamp wavelength: 280nm) exposure time. Both figures show a decreasing trend in absorbance intensity over time. At 0 min, the highest absorbance is observed. The absorbance intensity significantly drops over time, indicating a reduction in concentration of the compound due to photocatalytic activity. The results shown in Figure 3.4, and the photo degradation efficiency was calculated using the following equation:

$$\text{Photodegradation (\%)} = \frac{A_0 - A_t}{A_0} \times 100$$

Where :

A_0 : Absorbance at time $t = 0$ (before UV exposure)

A_t : Absorbance at time t (after UV exposure at 30, 60, 90, 120, 180 minutes)

demonstrate that incorporating Arabic gum polymer with secondary iron oxide enhanced the absorption rate from 42% to 72%, making this composite highly effective for applications in water treatment and purification.

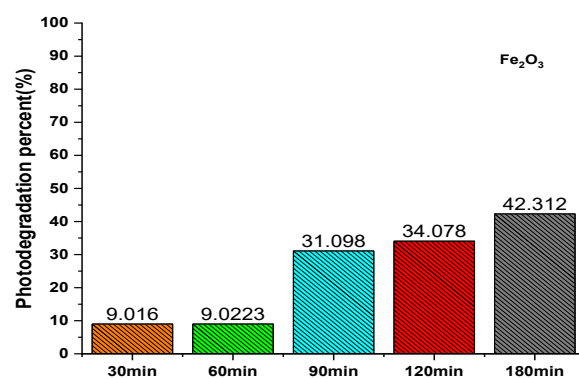
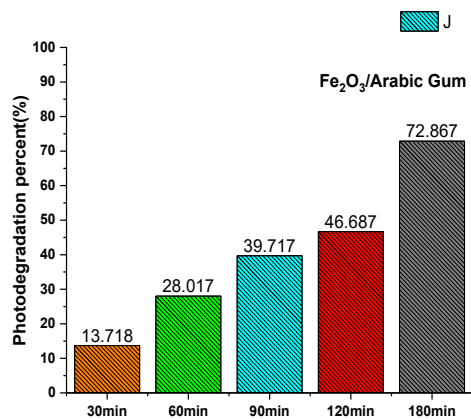
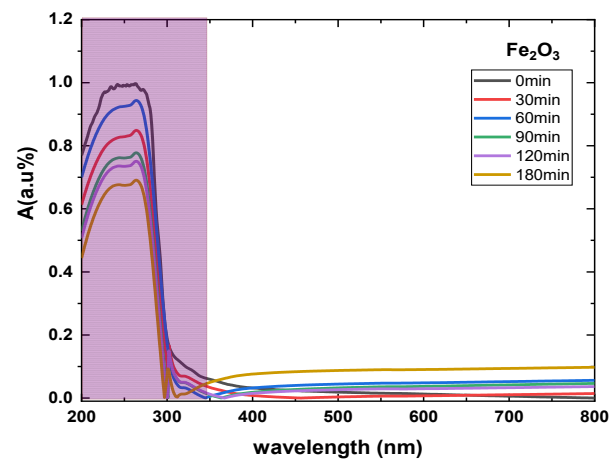
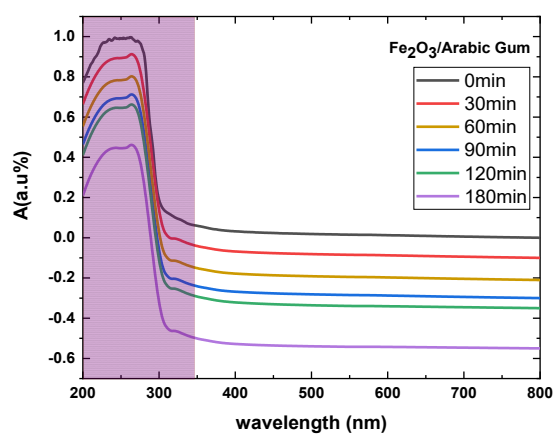


Figure.(3.4). UV spectra and photodegradation percent of samples

Conclusion

In this work, the characterization and application of iron oxide (Fe_2O_3) nanoparticles and their composite with Arabic gum polymer, prepared via mechanical ball milling, for enhanced water purification. The study was analyzing the magnetic properties of pure Fe_2O_3 and the Fe_2O_3 /Arabic gum composite using a VSM, revealing superparamagnetic behavior in both materials. Structural characterization via FTIR spectroscopy confirmed successful doping, as evidenced by the disappearance of the Fe-O vibration band at 468 cm^{-1} and the emergence of new peaks linked to interactions between the polymer and iron oxide. The photodegradation efficiency of the composite was tested under ultraviolet (UV) light using contaminated water samples from *Wadi Hanifa*, with exposure times ranging from 0 to 180 minutes. Remarkably, the Fe_2O_3 /Arabic gum composite demonstrated a significant increase in pollutant absorption, rising from 42% to 72% over 180 minutes, outperforming pure Fe_2O_3 . This enhancement was attributed to the Arabic gum's role in improving dispersion, increasing active surface area, and facilitating electron-hole pair separation under UV irradiation, which collectively boosted photocatalytic activity. The composite's ability to degrade organic pollutants highlights its potential as a sustainable, magnetically recoverable catalyst for water treatment, particularly in regions grappling with industrial or agricultural contamination. The ball milling method proved effective for synthesizing a homogeneous composite treatment systems. This research underscores the synergy between natural polymers and magnetic nanoparticles in addressing global water scarcity, offering a scalable, eco-friendly solution that combines the advantages of nanotechnology with renewable materials.

References

- [1] D. Callister William, & G. Rethwisch David. (2014). *Materials Science and Engineering: An Introduction* (9th ed.). Wiley
- [2] Issa, B., Obaidat, I. M., Albiss, B. A., & Haik, Y. (2013). Magnetic nanoparticles: Surface effects and properties related to biomedicine applications. In *International Journal of Molecular Sciences* (Vol. 14, Issue 11, pp. 21266–21305). <https://doi.org/10.3390/ijms141121266>
- [3] Balasubramanian Janani, Lemere Jack, Sudheer Khan S, & Agarwal Nisha. (2022). *Molecular and Laser Spectroscopy: advances and applications* (Gubta V, Ed.; Vol. 3). Elsevir.